The Journal of Neuroscience, October 15, 2002, 22(20):8891–8901

# Rapsyn Escorts the Nicotinic Acetylcholine Receptor Along the Exocytic Pathway via Association with Lipid Rafts

**Sophie Marchand,[1] Anne Devillers-Thiéry,[2] Stéphanie Pons,[2] Jean-Pierre Changeux,[2] and Jean Cartaud[1]**

[1]*Biologie Cellulaire des Membranes, Département de Biologie Cellulaire, Institut Jacques Monod, Centre National de la Recherche Scientifique, Universités Paris 6 et 7, 75251, Paris Cedex 05, France, and* [2]*Récepteurs et Cognition, Centre National de la Recherche Scientifique, Institut Pasteur, 75724, Paris Cedex 15, France*

The 43 kDa receptor-associated protein rapsyn is a myristoylated peripheral protein that plays a central role in nicotinic acetylcholine receptor (AChR) clustering at the neuromuscular junction. In a previous study, we demonstrated that rapsyn is specifically cotransported with AChR via post-Golgi vesicles targeted to the innervated surface of the *Torpedo* electrocyte (Marchand et al., 2000). In the present study, to further elucidate the mechanisms for sorting and assembly of postsynaptic proteins, we analyzed the dynamics of the intracellular trafficking of fluorescently labeled rapsyn in the transient-expressing COS-7 cell system. Our approach was based on fluorescence, time-lapse imaging, and immunoelectron microscopies, as well as biochemical analyses. We report that newly synthesized rapsyn associates with the *trans*-Golgi network compartment and traffics via vesiculotubular organelles toward the cell surface of COS-7 cells. The targeting of rapsyn organelles appeared to be mediated by a microtubule-dependent transport. Using co-transfection experiments of rapsyn and AChR, we observed that these two molecules codistribute within distal exocytic routes and at the plasma membrane. Triton X-100 extraction on ice and flotation gradient centrifugation demonstrated that rapsyn and AChR are recovered in low-density fractions enriched in two rafts markers: caveolin-1 and flotillin-1. We propose that sorting and targeting of these two companion molecules are mediated by association with cholesterol–sphingolipid-enriched raft microdomains. Collectively, these data highlight rapsyn as an itinerant vesicular protein that may play a dynamic role in the sorting and targeting of its companion receptor to the postsynaptic membrane. These data also raise the interesting hypothesis of the participation of the raft machinery in the targeting of signaling molecules to synaptic sites.

*Key words: rapsyn; nicotinic acetylcholine receptor; targeting; acylation; lipid rafts; exocytic pathway; COS cells*

The vertebrate neuromuscular junction ensures rapid and efficient synaptic transmission via the highly organized clustering of acetylcholine receptors (AChRs) at postsynaptic sites underlying the presynaptic area of neurotransmitter release. Several levels of regulatory mechanisms participate in the accumulation and maintenance of AChRs at newly formed synaptic sites of the neuromuscular junction, involving transcriptional regulation of the genes encoding the AChR subunits, clustering, and stabilization of the AChR via the cytoskeleton (for review, see Sanes and Lichtman, 1999; Schaeffer et al., 2001). Recent evidence demonstrated that additional posttranslational regulatory mechanisms consisting of an efficient sorting and direct targeting of AChR to the postsynaptic membrane also participate to ensure the proper supply of AChR at synaptic sites (Camus et al., 1998). Along this line, unraveling of the coordination between trafficking events of AChR and the various synapse-associated proteins is critical to the understanding of synaptogenesis at the neuromuscular junction.

The accumulation of AChR in the postsynaptic membrane is a complex process involving integral, cytoskeletal, and extracellular matrix components. Among the proteins of the postsynaptic cytoskeleton, the 43 kDa peripheral protein rapsyn (Sobel et al., 1977; for review, see Sanes and Lichtman, 1999) is of particular interest. Cotransfection experiments and rapsyn knock-out mice have demonstrated that rapsyn is required for AChR clustering (Froehner et al., 1990; Phillips et al., 1991a; Yu and Hall, 1994; Gautam et al., 1995). Rapsyn is myristoylated on its $NH_2$-terminal glycine during translation (Musil et al., 1988), and this modification is necessary for membrane binding (Phillips et al., 1991b; Ramarao and Cohen, 1998). In addition, a second membrane-binding signal required for stable membrane binding of myristoylated proteins (for review, see Resh, 1999) was recently proposed by molecular modeling of mouse rapsyn and consists of an N-terminal basic motif providing electrostatic interactions with acidic phospholipids (Ramarao et al., 2001).

The intrinsic feature of rapsyn to achieve stable membrane binding, together with the demonstration that several acylated proteins initially associate with intracellular membranes of the exocytic pathway to be subsequently targeted to the cell surface (Liu et al., 1994; Gonzalo and Linder, 1998; Bijlmakers and Marsh, 1999), supported our recent investigation of the intracellular routing of rapsyn in *Torpedo* electrocyte (Marchand et al., 2000). In this model system, we demonstrated that rapsyn is specifically cotransported with AChR via post-Golgi vesicles tar-

Received March 11, 2002; revised July 2, 2002; accepted July 15, 2002.

This work was supported by the Centre National de la Recherche Scientifique, the Universities Paris 6 and Paris 7, the Association Française contre les Myopathies (AFM), the Collège de France, and the European community. S.M. is a recipient of AFM. We thank Dr. J. Sanes for the generous gift of mouse rapsyn and AChR subunits plasmids. We also thank Agnès Trouillier and Gérard Géraud for expertise in confocal and video microscopies and Dr. Graça Raposo for advice on ultracryomicrotomy.

Correspondence should be addressed to Dr. Jean Cartaud, Biologie Cellulaire des Membranes, Institut Jacques Monod, Centre National de la Recherche Scientifique/Universités Paris 6 et 7, 2 Place Jussieu, F-75251, Paris Cedex 05, France. E-mail: cartaud@ijm.jussieu.fr.

geted to the postsynaptic membrane (Marchand et al., 2000). In the present article, to clarify the mechanisms for sorting and assembly of postsynaptic proteins, we further study the dynamics of intracellular trafficking of fluorescently labeled rapsyn protein in COS-7 cells. Additional cotransfection experiments of rapsyn and AChR subunit constructs enabled us to study the respective intracellular routing of these two major components of the neuromuscular junction. Our approach is based on fluorescence, time-lapse imaging, and immunoelectron microscopies, as well as biochemical analyses. We bring evidence that neosynthesized rapsyn–green fluorescent protein (GFP) associates in part with the *trans*-Golgi network (TGN) compartment and is initially targeted to tubulovesicular organelles en route to the cell surface of COS-7 cells. Videomicroscopy analysis further indicates that rapsyn-enriched organelles traffic via the microtubule network toward the cell cortex. In addition, our data support the notion that rapsyn and AChR codistribute within late exocytic compartments and are cotargeted to the plasma membrane. Finally, we propose that sorting and targeting of these two companion molecules are mediated by association with cholesterol–sphingolipid-enriched raft microdomains.

## MATERIALS AND METHODS

*Antibodies and reagents*. Rabbit polyclonal anti-mannose-6-phosphate receptor (M6PR) antibody was a generous gift from Dr. B. Hoflack (Institut Pasteur, Lille, France). Rabbit polyclonal anti-Ras-related GTPase 5a (Rab5a; S-19) and anti-caveolin-1 (N-20) antibodies were from Santa Cruz Biotechnology (Santa Cruz, CA), sheep anti-human TGN46 was from Serotec, mouse monoclonal anti-$\alpha$ tubulin antibody was purchased from Amersham Biosciences (Little Chalfont, UK), a mixture of mouse monoclonal anti-GFP antibodies (clones 7.1 and 13.1) was from Roche (Indianapolis, IN), and mouse monoclonal anti-AChR $\alpha$-subunit (clone 26) and anti-flotillin-1 antibodies were obtained from Transduction Laboratories (Lexington, KY). The following reagents and antibodies were used for immunofluorescence detection: RITC-conjugated $\alpha$-bungarotoxin was from Molecular Probes (Eugene, OR), and tetramethylrhodamine isothiocyanate (TRITC)-conjugated wheat germ agglutinin (WGA) and filipin were purchased from Sigma (St. Louis, MO).

Brefeldin A (BFA), nocodazole, and methyl-$\beta$-cyclodextrin (M$\beta$CD) were obtained from Sigma. Okadaic acid was obtained from Calbiochem (Bad Soden, Germany).

*Rapsyn and AChR constructs*. Full-length cDNAs coding for mouse rapsyn and AChR subunits (Phillips et al., 1991a) were kindly provided by Dr. J. R. Sanes (Washington University, St. Louis, MO). The GFP was fused to the C-terminal domain of rapsyn, thus enabling N-terminal myristoylation necessary for membrane binding (Ramarao and Cohen, 1998). To generate the C-terminal enhanced green fluorescent protein (EGFP) fusion rapsyn construct and the $\alpha$, $\beta$, $\gamma$, and $\delta$ AChR subunit constructs, PCR was used to introduce appropriate restriction enzyme sites on the 5′ and 3′ termini of rapsyn and AChR subunit cDNAs. For the rapsyn construct, the PCR product was then cloned in frame with the GFP coding sequence of the pEGFP-N1 vector (Clontech, Cambridge, UK). For AChR subunits constructs, the PCR products were cloned within the pcDNA3 vector (Invitrogen). All constructs were verified by sequencing.

*Cell culture and transient transfection*. COS-7 cells (African Green Monkey kidney) were maintained in 10% fetal bovine serum in Roswell Park Memorial Institute (RPMI) 1640 medium (Life Technologies, Eggenheim, Germany) with 100 U/ml penicillin and streptomycin. Cells were maintained at 37°C in a humidified atmosphere containing 5% $CO_2$. The day before transfection, COS-7 cells were trypsinized and $2 \times 10^5$ or $1.5 \times 10^6$ cells were plated into one well of a six-well plate for immunofluorescence analysis or into one 100 mm dish for biochemical studies, respectively. Cells were transfected with Fugene 6 reagent according to the manufacturer's instructions (Roche). The routine cDNA plasmid concentrations for rapsyn and AChR subunits were $\alpha$, 0.5 $\mu$g/ml; $\beta$, $\gamma$, and $\delta$, 0.25 $\mu$g/ml; and rapsyn, 0.25 $\mu$g/ml. Assays were performed 12, 24, or 48 hr later.

*Quantification of cell-surface AChR*. The quantification of AChR expressed at the cell surface of transfected COS-7 cells was achieved using $^{125}$I-$\alpha$-bungarotoxin binding protocol. Cells expressing AChR alone or AChR and rapsyn for 1 d were washed rapidly with PBS at room temperature and then incubated for 1 hr at 4°C with PBS containing BSA (1 mg/ml) and 5 nM $^{125}$I-$\alpha$-bungarotoxin (150 Ci/mmol; Amersham Biosciences). Cells were washed three times at 4°C with PBS and lysed in PBS containing 1% SDS at 37°C. $^{125}$I radioactivity was counted for 1 min with an MR480 gamma counter (Kontron Elektronik, Eching, Germany). Background obtained by $^{125}$I-$\alpha$-bungarotoxin binding after saturation with 1 $\mu$M nicotine was subtracted. Each experiment was done in triplicate.

*Immunofluorescence microscopy*. Transfected COS-7 cells grown on polylysine-treated glass coverslips were washed twice with PBS and fixed for 20 min at room temperature with 3% paraformaldehyde in 0.1 M phosphate buffer (PB), pH 7.4. Fixed cells were rinsed with PBS, and when permeabilization was needed, cells were incubated with 0.1% Triton X-100 for 5 min at room temperature and then washed with PBS. After preincubation during 30 min at room temperature in PBS containing 4% BSA and 1% fish gelatin, cells were incubated for 2 hr with primary antibodies (anti-AChR $\alpha$-subunit, 1:100; anti-CTR433, 1:50; anti-M6PR, 1:500; anti-Rab5a, 1:200; anti-TGN46, 1:400; anti-$\alpha$-tubulin, 1:400) at room temperature in PBS containing 0.4% BSA and 0.1% fish gelatin (medium 1). Cells were washed four times for 5 min in PBS and incubated with secondary fluorophore-conjugated antibodies (Jackson ImmunoResearch, West Grove, PA) in medium 1 for 30 min at room temperature. RITC-conjugated bungarotoxin (1 $\mu$g/ml; Molecular Probes), TRITC-conjugated WGA (5 $\mu$g/ml; Sigma), and 4′,6′-diamidino-2-phenylindole (DAPI; 1 $\mu$g/ml) were added with the secondary antibodies to label AChRs, Golgi apparatus, and nuclei, respectively. After three washes for 5 min in PBS, coverslips were mounted in Citifluor (Citifluor Ltd., London, UK). Micrographs were taken with a Leica DMR microscope (Heidelberg, Germany) equipped with a Micro Max cooled charge-coupled device (CCD) camera (Princeton Instruments, Trenton, NJ). Confocal laser scanning microscopy was performed using a TCS-4D confocal imaging system (Leica instrument), equipped with a 63× objective (plan apo; numerical aperture = 1.4). For FITC and CY3 excitation, an Argon-Krypton ion laser adjusted at 488 and 568 nm, respectively, was used. The confocal system was adjusted to allow a field depth of ~0.5 $\mu$m. Digital images were captured using MetaView Imaging System (Universal Imaging Corp., West Chester, PA) and arranged using Adobe Systems PhotoShop v5.0 (San Jose, CA).

The effect of nocodazole, BFA, and okadaic acid on the distribution of rapsyn and AChR was studied by adding nocodazole, BFA, or okadaic acid to the culture medium at final concentrations of 10 $\mu$g/ml, 5 $\mu$g/ml, or 0.5 $\mu$M, respectively. Cells were incubated at 37°C for the overall time of rapsyn–GFP expression for nocodazole, 2 hr for BFA, and 1 hr for okadaic acid, fixed with 3% paraformaldehyde, and handled for immunofluorescence as described above.

Filipin, a fluorescent polyene antibiotic, was used to detect free cholesterol through interactions with a free 3$\beta$-hydroxyl group (Muller et al., 1984). For filipin detection, cells were fixed, permeabilized, and blocked as described above, and incubated for 2 hr at room temperature with 0.5 ml of medium 1 containing 50 $\mu$g/ml filipin added from a stock solution in dimethylsulfoxide (final concentration 0.2% v/v). After several washes, coverslips were mounted, and fluorescence detection of filipin was done with an ultraviolet filter (Leica).

Depletion of cellular cholesterol was performed using the cholesterol-depleting drug M$\beta$CD. After 1 d of expression, cells were depleted of cholesterol by incubation for 1 hr in 10 or 20 mM M$\beta$CD dissolved in serum-free RPMI at 37°C. Coverslips were then washed, fixed, blocked, and processed for immunofluorescence and filipin fluorescent detection.

*Ultracryomicrotomy and immunoelectron microscopy*. COS-7 cells were fixed with 3% paraformaldehyde in 0.1 M PB, pH 7.4, overnight at 4°C. Cell pellets were washed for 1.5 hr in PB containing 50 mM glycine at 4°C to quench free aldehyde groups, washed three times for 5 min in PB at 4°C, embedded in 7% (w/v) gelatin, and infused for 2 hr in 2.3 M sucrose in PB (Raposo et al., 1997). Mounting gelatin blocks were frozen in liquid nitrogen, and 40–60 nm ultrathin cryosections were prepared with an Ultracut ultracryomicrotome (Leica) and collected with 2% (v/v) methylcellulose and 2.3 M sucrose (Liou et al., 1996). Ultrathin cryosections were immunogold labeled as described (Slot et al., 1991; Raposo et al., 1997) with the use of antibodies coupled to 10 nm gold particles (AuroProbe EM; Amersham Biosciences). All sections were observed

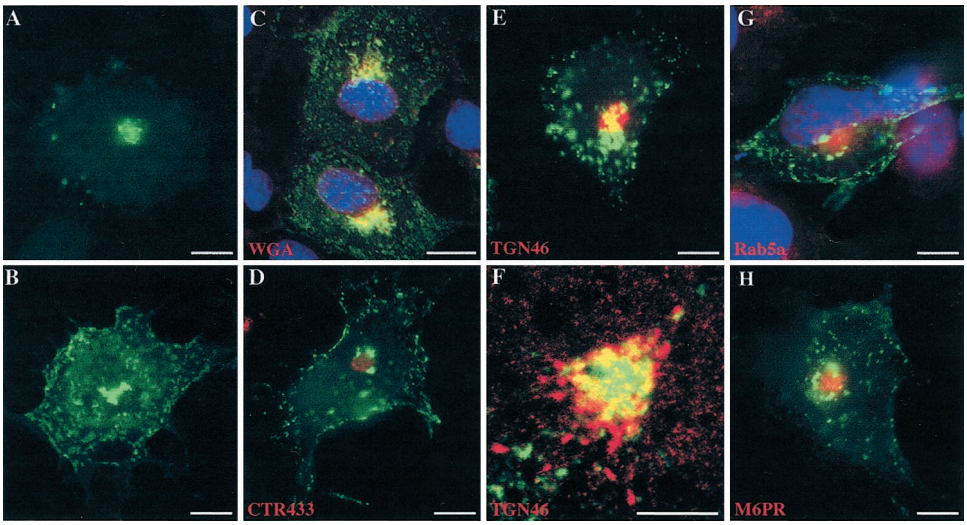


*Figure 1.* Subcellular targeting of rapsyn–GFP to exocytic compartments in COS-7 cells. Cells were transfected with rapsyn fused to GFP (rapsyn–GFP) as described in Materials and Methods. Twelve to 24 hr after transfection, cells were fixed and handled for immunofluorescence using TRITC-conjugated WGA (*C*), monoclonal anti-CTR433 antibody (*D*), monoclonal anti-TGN46 antibody (*E*, *F*), polyclonal anti-Rab5a (*G*), or anti-M6PR antibodies (*H*). In some experiments, DAPI staining was performed to localize the nuclei. At early expression times, rapsyn–GFP mostly localized in a juxtanuclear region (*A*). At later expression times, rapsyn–GFP distributed in clusters at the plasma membrane, as well as in the juxtanuclear region, and in a dot-like pattern within the cytoplasm (*B*). Rapsyn–GFP fluorescence overlapped partially with WGA staining (*C*) and with the *trans*-Golgi network marker TGN46 (*E*). At higher magnification, confocal analysis confirmed the codistribution of rapsyn–GFP with TGN46 (*F*). Rapsyn–GFP did not overlap significantly with the markers of CTR433 (*D*) and the early and late endosomal compartments Rab5a and M6PR, respectively (*G*, *H*). Scale bars: *A–E*, *G*, *H*, 10 μm; *F*, 5 μm.

with a Philips CM12 electron microscope operating at 80 keV. Micrographs were taken on Eastman Kodak (Rochester, NY) EM 4489 electron microscope films.

*Time-lapse video microscopy of living cells*. COS-7 cells were transfected with rapsyn–GFP as described above. Cells were grown on uncoated 12 mm coverslip dishes and transferred 24 hr later to medium RPMI without red phenol before viewing. For drug experiments, cells were incubated with nocodazole (10 μg/ml) 4 hr after transfection and then left in this medium until analysis. Cells were observed in an open chamber at 37°C, 5% $CO_2$, with an inverted microscope (Leica DMIRBE) equipped for epifluorescence and phase-contrast microscopy. Data were acquired with a cooled CCD Pentamax camera (Princeton Instruments, Inc.) driven by Metamorph software and stored as 16 bit digital images. Fluorescent images were taken every 20 sec. The video sequences were analyzed and processed using Metamorph Imaging System (Universal Imaging Corp.).

*Flotation experiments and Western blotting*. Transfected COS-7 cells grown to near confluence in 100 mm dishes were used to prepare detergent–resistant membranes. After two washes with ice-cold PBS, cells from each confluent dish were scraped into 2 ml of 2-[*N*-morpholino]ethanesulfonic acid (MES), pH 6.5, 0.15 M NaCl] containing 1% (w/v) Triton X-100, and solubilized for 30 min on ice. Homogenization was performed with the use of 10 strokes of a tight-fitting Dounce homogenizer for Triton X-100-containing samples. The homogenates were adjusted to 40% sucrose in MES, placed at the bottom of an ultracentrifuge tube, and overlaid with 4 ml of 30% sucrose and 4 ml of 5% sucrose. Antiproteases (1 mM leupeptin, 1 mM pepstatin, 1 mM phenylmethylsulfonyl fluoride, 0.5 mg/ml aprotinin, and 1 mM benzamidin) were added throughout the experiment. Gradients were centrifuged at 39,000 rpm for 16–20 hr at 4°C in a SW41 Ti rotor (Beckman Instruments, Fullerton, CA). A light-scattering band was observed at the 5–30% sucrose interface corresponding to the detergent-resistant membranes. Twelve 1 ml fractions were collected from the top of the tubes, precipitated with 9% trichloroacetic acid for 30 min, and washed with 80% cold acetone.

Proteins from the various membrane preparations were separated on 12% SDS-PAGE (Mini Protean II; Bio-Rad, Richmond, CA). After separation, proteins were electrotransferred onto nitrocellulose paper (Schleicher & Schuell, Dassel, Germany) according to Towbin et al. (1979). Immunoblot experiments were performed as described elsewhere (Cartaud et al., 1993). Detection of the signal was achieved through a chemiluminescent reaction (enhanced chemiluminescence; Amersham Biosciences) using x-ray films (Fuji Photo Film Co., Tokyo, Japan). Antibody dilutions were 1:2000 for anti-GFP, 1:400 for anti-AChR α subunit, 1:500 for anti-caveolin-1, and 1:400 for anti-flotillin-1.

## RESULTS

### Neosynthesized rapsyn–GFP associates with the *trans*-Golgi network when heterologously expressed in COS-7 cells

To define cellular processes that mediate rapsyn trafficking to the plasma membrane, we first analyzed the subcellular distribution of rapsyn–GFP transfected in COS-7 cells. At early expression times (12 hr), rapsyn–GFP was mostly localized in a juxtanuclear region that resembled, in both localization and appearance, the Golgi complex (Fig. 1*A*). At later expression times (24 hr), as expected, rapsyn is distributed in clusters at the plasma membrane and within the cytoplasm in the juxtanuclear region and in a dot-like pattern (Fig. 1*B*). To determine whether this transient juxtanuclear localization of rapsyn corresponded to a specific organelle, in particular the Golgi apparatus, we performed immunofluorescence staining of the transfected cells with various markers of the compartments of the exocytic and endocytic pathways: WGA (Tartakoff and Vassalli, 1983) as a marker of the Golgi apparatus, including the *trans*-Golgi network; CTR433 as a marker of the *medial*-Golgi cisternae (Jasmin et al., 1989); TGN46 as a marker of the TGN (Ponnambalam et al., 1996); and Rab5a and M6PR as markers of early and late endosomal compartments, respectively (Griffiths et al., 1988; Chavrier et al., 1990). As shown by immunofluorescence and confocal analyses, rapsyn–GFP fluorescence overlapped, although partially, with that of the WGA (Fig. 1*C*) and TGN46 (Fig. 1*E*,*F*). Conversely, rapsyn did not overlap significantly with the *medial*-Golgi compartments (CTR433) (Fig. 1*D*) and the early and late endosomes markers Rab5a (Fig. 1*G*) and M6PR (Fig. 1*H*), respectively. These observations suggest that neosynthesized rapsyn–GFP associates with the exocytic pathway, within a distal subcompartment of the Golgi apparatus, the *trans*-Golgi network. At later expression times, rapsyn was less concentrated in this structure and started to accumulate within the cytoplasm and at the plasma membrane.

To confirm that neosynthesized rapsyn–GFP specifically associates with the TGN compartment, we performed drug experiments and took advantage of the differential effects of BFA and

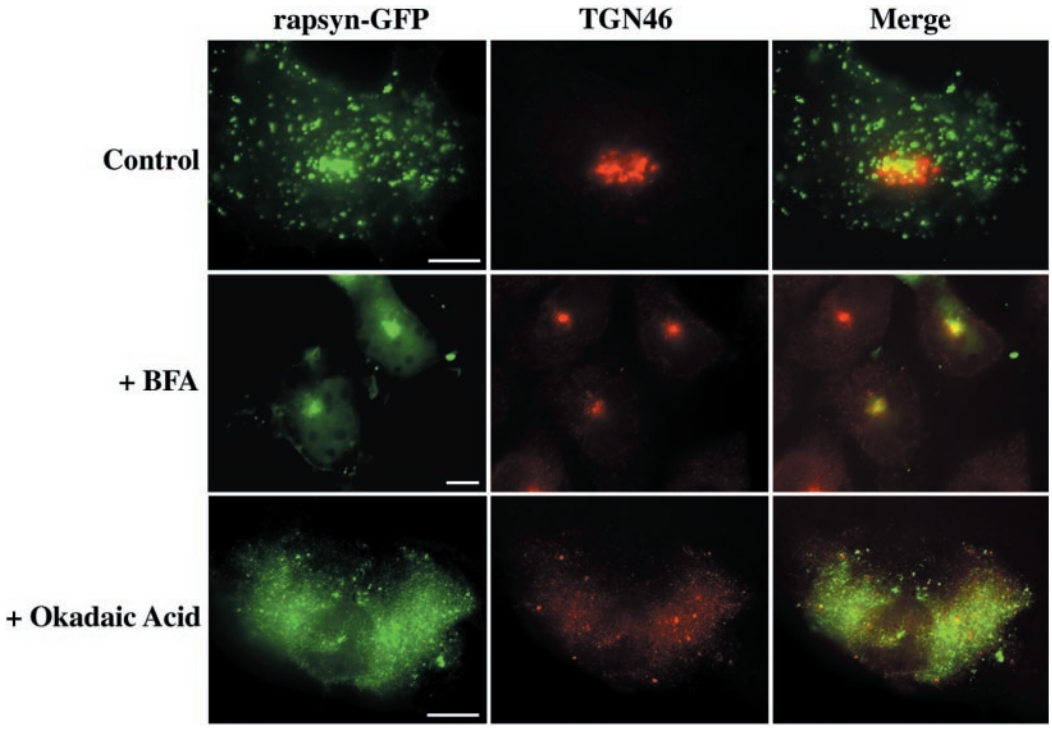


*Figure 2.* Rapsyn–GFP localizes to the *trans*-Golgi network. COS-7 cells were transfected with rapsyn–GFP. One day later, cells were incubated in either the absence (*Control*) or presence of 5 μg/ml brefeldin A for 2 hr (*+BFA*) or 0.5 μM okadaic acid for 1 hr (*+Okadaic Acid*). The cells were fixed and labeled with the TGN46 monoclonal antibody and observed in the fluorescence microscope. Rapsyn–GFP remained associated with condensed TGN in conditions in which the Golgi apparatus was disrupted by BFA. After okadaic acid treatment, which disrupts the entire Golgi complex, including the TGN, rapsyn–GFP-associated structures were dispersed within the cytoplasm. Scale bar, 10 μm.

okadaic acid on the Golgi complex. The fungal metabolite BFA is known to inhibit coat formation of the Golgi membranes, thereby disrupting the cisternal stacks leading to a redistribution of the *cis*-, *medial*-, and *trans*-cisternae into the endoplasmic reticulum (ER), leaving the TGN to coalesce into a more spherical mass near the centrioles (Banting and Ponnambalam, 1997; Chardin and McCormick, 1999; Watson and Pessin, 2000). In contrast, okadaic acid disrupts the entire Golgi complex, including the TGN (Horn and Banting, 1994). On BFA treatment, we observed a concentrated spherical distribution of rapsyn–GFP similar to that of the TGN46 marker and consistent with a TGN localization (Fig. 2, *+BFA*). Okadaic acid treatment induced a dispersion of rapsyn–GFP fluorescence consistent with the disruption of the entire Golgi complex, including the TGN (Fig. 2, *+Okadaic Acid*). Consequently, neosynthesized rapsyn–GFP localizes initially to the TGN in COS-7 cells.

### Rapsyn–GFP traffics via pleiomorphic vesiculotubular carriers to the plasma membrane

To verify that the large rapsyn–GFP fluorescent dots in COS-7 cells were not caused by mere protein aggregation and to define the ultrastructure of rapsyn–GFP-enriched carriers, we performed immunogold electron microscopy of COS-7 cells 24 hr after transfection. Using an anti-GFP monoclonal antibody detected with 10 nm colloidal gold-conjugated IgGs, we showed that rapsyn decorated the cytosolic surface of numerous intracellular tubulovesicular membranes of various size and shape, often accumulated within the juxtanuclear region (Fig. 3). No gold particle aggregates were observed, confirming that rapsyn–GFP molecules selectively associate with membranous structures. These EM data are in agreement with our conclusion that rapsyn–GFP associated with TGN-derived membranes.

Then, we used videomicroscopy to monitor the dynamics of rapsyn–GFP-enriched organelles operating from the *trans*-Golgi network to the cell surface in living COS-7 cells. In the first time-imaging sequence (Fig. 4), we observed large tubulovesicular rapsyn–GFP-containing organelles that merged with each other while moving toward the cell surface and were finally delivered to the plasma membrane presumably by fusing with it (Fig. 4*B*, *arrow* in *panel 4*). Fluorescence then vanished as rapsyn spread out along the membrane (Fig. 4*B*, *panel 6*). These observations are reminiscent of the trafficking of Golgi-derived vesicular transport intermediates for transmembrane and peripheral proteins (Sciaky et al., 1997; El-Husseini et al., 2000). Our observations agree with electron microscopy analysis by supporting the pleiomorphic feature of rapsyn–GFP carriers. Moreover, the outward movement of rapsyn–GFP organelles toward the cell surface illustrates their exocytic origin.

### Role of the microtubular network in the localization and transport of rapsyn–GFP in COS-7 cells

Besides its key role in the spatial organization of the cell biosynthetic machinery, the microtubular network is suggested to facilitate transport of post-Golgi carriers toward the cell surface (Mays et al., 1994; Lafont and Simons, 1996). To uncover the putative role of microtubular cytoskeleton in the intracellular localization of rapsyn-associated organelles and the dynamics of rapsyn transport to the cell surface, we used immunofluorescence analyses of the distribution of rapsyn–GFP versus the microtubular organization, as well as videomicroscopy. At the early

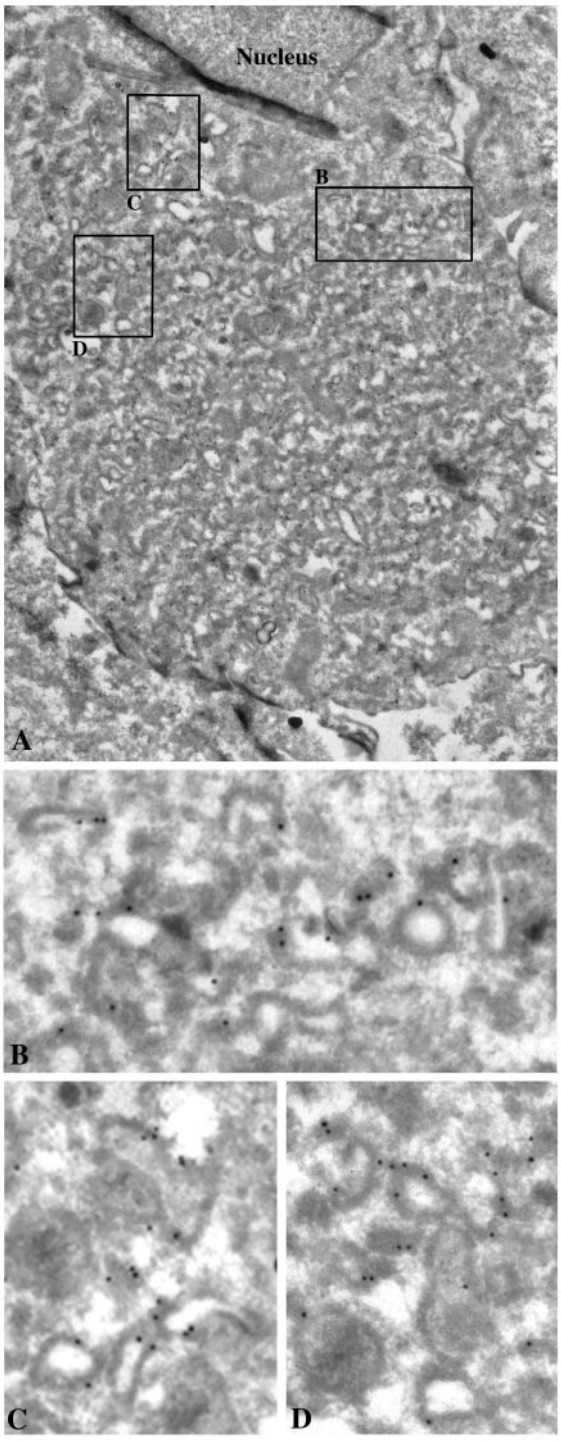


*Figure 3.* Immunogold localization of rapsyn–GFP in COS-7 cells. Ultrathin cryosections of transfected COS-7 cells were immunolabeled with 10 nm of gold-conjugated monoclonal anti-GFP antibody and observed by electron microscopy. Rapsyn was associated with the cytoplasmic surface of numerous intracellular tubulovesicular organelles (details in *B–D*) often accumulated within the juxtanuclear region (*A*). Magnifications: *A*, 10,000×; *B–D*, 35,000×.

expression time of rapsyn–GFP, juxtanuclear rapsyn–GFP appeared in close proximity to the microtubular-organizing center (MTOC) (Fig. 5*A*, *arrow*). At later expression times (2 d after transfection), rapsyn–GFP fluorescence distributed as numerous

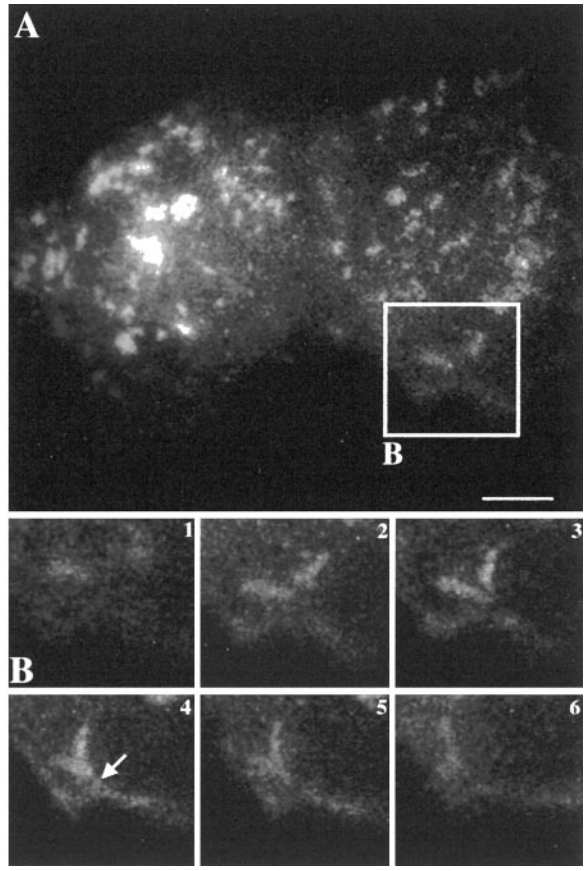


*Figure 4.* Dynamics of intracellular trafficking of rapsyn–GFP by videomicroscopy. *A*, The COS-7 cell transfected with rapsyn–GFP was analyzed by three-dimensional videomicroscopy after 24 hr of expression. *B*, Time series imaging of the selected area of the cell in *A*. Tubulovesicular rapsyn-enriched organelles fused together while moving toward the cell surface and with the plasma membrane (*arrow*). The signal then vanished as rapsyn spread out along the membrane. Time intervals between frames were 20 sec. Scale bar, 10 μm.

organelles that are concentrated around the MTOC (Fig. 5*B*, *arrow*), as well as underlying the cell cortex (Fig. 5*B*, *arrowheads*). Rapsyn–GFP clusters were also detected at the plasma membrane. Confocal analysis at higher magnification suggested an association of rapsyn–GFP-containing structures with microtubules (Fig. 5*C*). In addition to the microtubular-disrupting drug nocadozole, we observed a dramatic redistribution of rapsyn–GFP transporters as small fluorescent structures dispersed within the cytoplasm of COS-7 cells (Fig. 5*D*). The time-imaging sequence in Figure 6 illustrates the movement of a rapsyn–GFP organelle originating from the juxtanuclear region. The organelle depicted by the arrow moved straight from the cell center to the periphery and then tangentially to the cell surface (Fig. 6*B*). Both the speed of the transport (~0.2 μm/sec) and the linear trajectory were consistent with a microtubule-mediated movement. Moreover, the trajectory of rapsyn–GFP transporters is in agreement with the organization of the tubulin-based cytoskeleton radiating from the MTOC toward the cell periphery and underlying the plasma membrane (Fig. 6*C*). To confirm the participation of microtubules in rapsyn trafficking, cells were treated with the microtubular-disrupting drug nocodazole. As expected, the movement of rapsyn–GFP-containing organelles was nearly completely inhibited by the drug (data not shown), indicating that their long-range displacement requires the microtubule network.

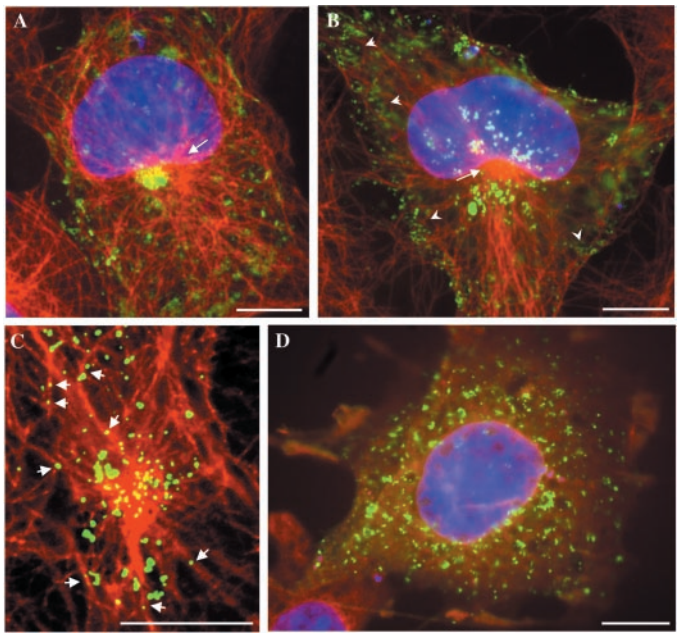


*Figure 5.* Rapsyn–GFP localization is dependent on the integrity of the microtubular network. COS-7 cells expressing rapsyn–GFP were fixed and handled for immunofluorescence microscopy using monoclonal anti-α-tubulin antibody. *A*, In cells starting to express rapsyn–GFP (24 hr), TGN-associated rapsyn–GFP appeared in close proximity with the MTOC (*arrow*). *B*, At later expression times (typically 2 d), rapsyn–GFP distributed as numerous organelles surrounding the MTOC and underlying the cell cortex (*arrowheads*). *C*, Confocal analysis suggested the association of rapsyn–GFP carriers with microtubules (*arrows*). *D*, Depolymerization of microtubules by nocodazole disrupted juxtanuclear and cortical distributions of rapsyn–GFP. *A*, *B*, *D*, DAPI staining was performed to localize the nuclei. Scale bars, 10 μm.

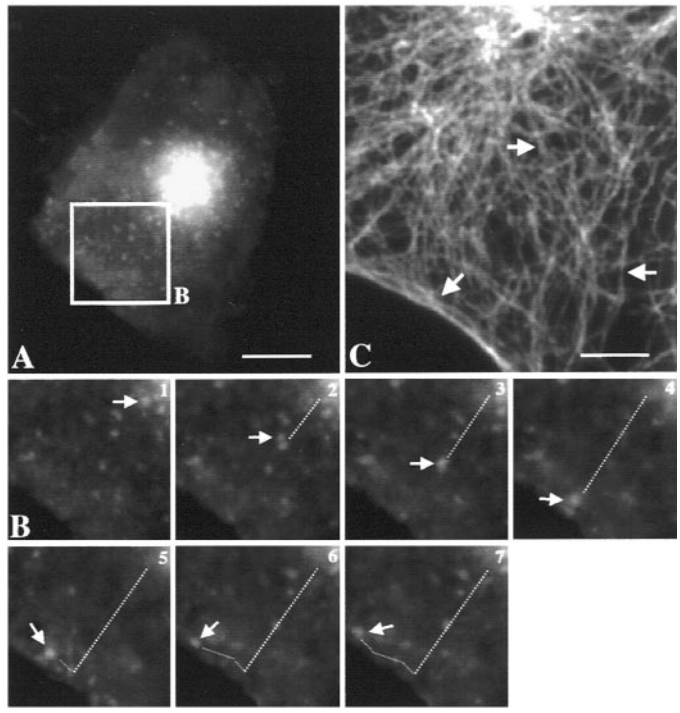


*Figure 6.* Dynamics of intracellular trafficking of rapsyn–GFP by videomicroscopy: role of microtubules. *A*, The COS-7 cell transfected with rapsyn–GFP was analyzed by three-dimensional videomicroscopy after 24 hr of expression. *B*, Time series imaging of the selected area of the cell in *A*. The organelle indicated by the *arrow* moved straight from the cell center to the periphery and then tangentially to the cell surface. Both the velocity (~0.2 μm/sec) of the transport and the linear trajectory suggested a microtubule-guided movement. The trajectory of rapsyn–GFP transporters is consistent with the microtubular organization (*C*) radiating from the MTOC (*arrow*) toward the cell periphery and underlying the plasma membrane (*arrows*). Intervals between frames are 20 sec. Scale bars: *A*, 10 μm; *C*, 5 μm.

## Rapsyn and AChR are cotargeted along the exocytic pathway in COS-7 cells

In a previous study, we investigated the intracellular routing of rapsyn and AChR in *Torpedo* electrocytes. We demonstrated that the two molecules might be associated early in the exocytic pathway and are cotargeted via common vesicular carriers to the postsynaptic membrane (Marchand et al., 2000). To clarify the molecular mechanisms involved in the targeting of rapsyn versus AChR, we performed cotransfection experiments of cDNAs for rapsyn–GFP and the four subunits of the mouse AChR in COS-7 cells followed by immunofluorescence microscopy. As observed previously (Froehner et al., 1990; Phillips et al., 1991a; Yu and Hall, 1994; Ramarao and Cohen, 1998) in cells expressing only AChR, receptors were diffusely distributed on the cell surface (Fig. 7*H*,*I*). When rapsyn–GFP was cotransfected along with AChR subunits, a different pattern of staining was seen in which the AChR redistributed and appeared in coclusters with rapsyn at the cell surface (Fig. 7). Intracellularly, AChR and rapsyn exhibited partially similar patterns of distribution. AChR staining was distributed within perinuclear, juxtanuclear, and more distal cytoplasmic compartments consistent with its biosynthetic routing along endoplasmic reticulum, Golgi apparatus, the *trans*-Golgi network, and cytoplasmic transport organelles, respectively (Fig. 7*A*,*D*). Conversely, as already observed in cells expressing rapsyn alone, rapsyn staining associated only with the juxtanuclear compartment likely corresponding to TGN (Fig. 7*B*,*E*,*G, arrowheads*) (also see Figs. 1, 2) and with cytoplasmic organelles (Fig. 7*G*). These observations indicate that in COS-7 cells, rapsyn escorts AChR within distal compartments of the exocytic pathway, and therefore these two proteins are cotargeted to the cell surface.

To answer the question of to what extent does cotransfection with rapsyn change the intracellular distribution of AChR, we compared cells individually transfected with AChR alone or cotransfected with rapsyn. In cells transfected with AChR subunits in the absence of rapsyn, no difference in the intracellular distribution of AChR was observed compared with cotransfected cells (Fig. 7, compare *A*,*D* with *H*,*I*), indicating that rapsyn did not change the intracellular distribution of AchR, at least with respect to those organelles thought to be important for transport to the surface. To further analyze the potential role of rapsyn in AChR vesicular trafficking, we also evaluated the amount of AChR present at the cell surface. Compared with cells expressing AChR alone, the number of toxin-binding sites at the cell surface (see Materials and Methods) was slightly increased ($\times 1.5 \pm 0.5$; $n = 5$) after cotransfection with rapsyn. This observation could be accounted for by the known role of rapsyn in the metabolic stabilization of surface AChR (Z. Z. Wang et al., 1999) rather than by a facilitation of AChR delivery by rapsyn. This conclusion is in agreement with the present fluorescence experiments.

## The intracellular routing of rapsyn and AChR is mediated by their association with lipid raft microdomains

Cholesterol–sphingolipid-enriched microdomains or lipid rafts are part of the machinery ensuring correct intracellular traffick-

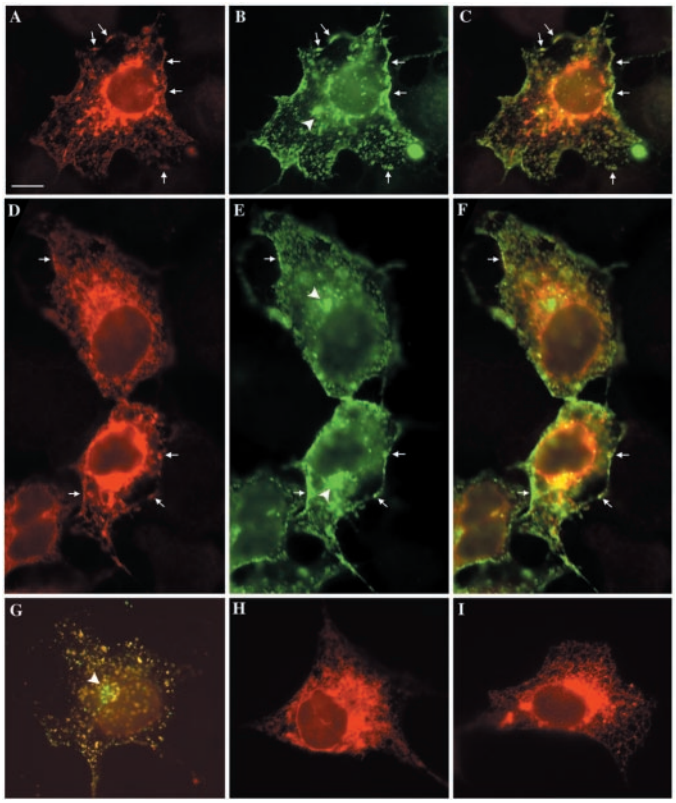


*Figure 7.* Distributions of AChR and rapsyn–GFP in the exocytic pathway in COS-7 cells. Cells transfected with AChR α, β, γ, and δ subunit constructs or cotransfected with rapsyn–GFP and AChR subunits constructs were fixed, permeabilized with 0.1% Triton X-100, and processed for immunofluorescence using anti-AChR α-subunit antibody or TRITC-conjugated α-bungarotoxin. AChR (*A*, *D*) and rapsyn (*B*, *E*) colocalized at the cell surface and partially within intracellular compartments (*C–F*). Intracellularly, AChR distributed within the entire exocytic pathway, whereas rapsyn–GFP fluorescence was observed only in distal compartments, including the TGN (*B*, *E*, *arrowheads*; also see Figs. 1, 2) and cytoplasmic organelles (*G*). In cells transfected only with AChR subunits, a similar intracellular distribution was observed (*H*, *I*). Note that no AChR clusters were present at the cell surface (*H*, *I*) at variance with cells cotransfected with rapsyn–GFP (*A*, *D*, *arrows*). *A*, *D*, *H*, *I*, AChR labeling with anti-AChR α-subunit antibody; *B*, *E*, rapsyn–GFP; *C*, *F*, *G*, double-labeling AChR/rapsyn–GFP. *G*, AChR labeling was achieved by α-bungarotoxin. Scale bar, 10 μm.

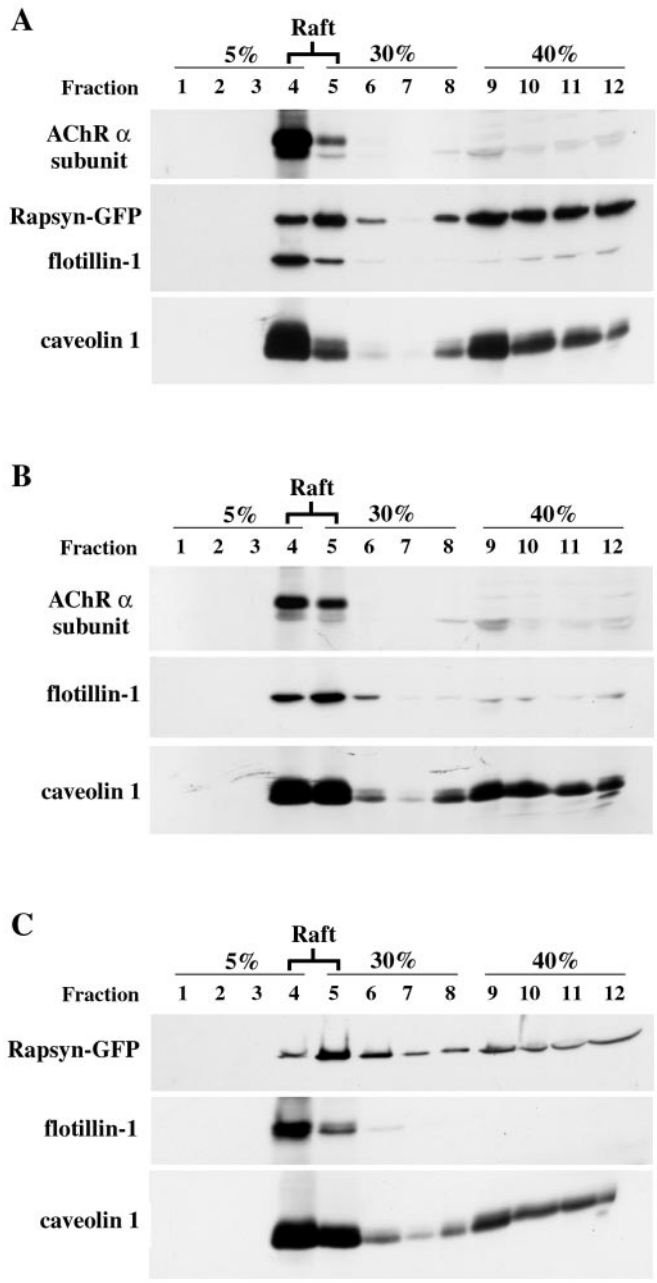


*Figure 8.* Raft fractionation of rapsyn–GFP and AChR in COS-7 cells. Cells transiently cotransfected with rapsyn–GFP and AChR subunits (*A*) or separately with AChR subunits (*B*) or rapsyn (*C*) were subjected to subcellular fractionation by extraction with 1% (w/v) Triton X-100 on ice. Cell lysates were separated by ultracentrifugation on discontinuous sucrose density gradients. Fractions collected from the top of the gradient were separated by SDS-PAGE (12% acrylamide) and analyzed by immunoblotting (see Materials and Methods). The distributions of rapsyn–GFP and AChR α subunit along the gradient were compared with those of caveolin-1 and flotillin-1, two endogenous markers of lipid rafts. AChR α subunit (49 kDa) and rapsyn–GFP (70 kDa) fractionated mostly in the low-density caveolin-1(26 kDa)/flotillin-1(52 kDa)-enriched raft fractions (*lanes 4*, *5*).

ing of proteins and lipids. By governing protein–protein and protein–lipid interactions, these domains selectively incorporate or exclude proteins and therefore have been proposed to function as membrane platforms for the assembly of signaling complexes and for the sorting of molecules to particular cellular structures (for review, see Ikonen, 2001). Along this line, we wanted to address the question of whether rapsyn and nicotinic AChR associate with lipid rafts in COS-7 cells. Lipid raft microdomains are uniquely resistant to extraction with cold, nonionic detergent, such as Triton X-100 treatment, and raft-associated proteins, by virtue of their continued association with raft lipids, exhibit a buoyant density that allows them to be separated from nonraft membrane proteins by flotation on density gradients. After 48 hr expression, cells transfected with rapsyn–GFP and/or AChR four subunit constructs were extracted on ice in a buffer containing 1% (w/v) Triton X-100 (see Materials and Methods). After flotation on discontinuous sucrose gradients, fractions were collected, and the distribution of rapsyn–GFP and AChR α subunit was studied by Western blot analysis using caveolin-1 and flotillin-1 as endogenous protein markers of lipid rafts. As expected, caveolin-1 and flotillin-1 were concentrated at the 5–30% sucrose interface referred to as the light raft-containing fractions (Fig. 8, *lanes 4*, *5*), with some caveolin present in the soluble high-density fractions

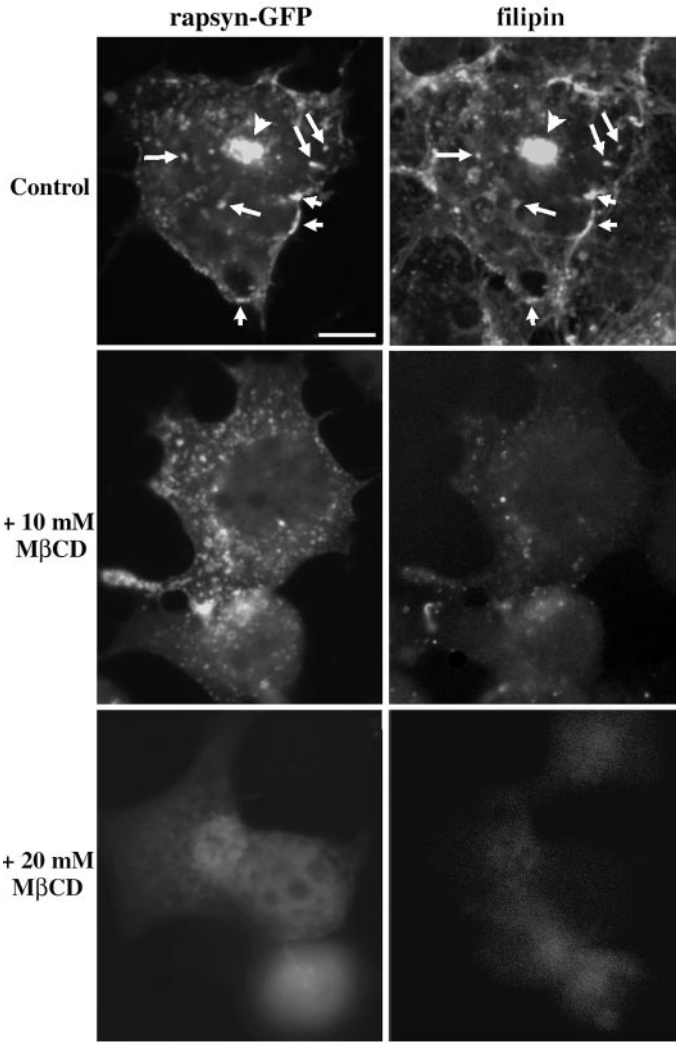


*Figure 9.* Role of cholesterol in the distribution of rapsyn-GFP in COS-7 cells. Cells transfected with plasmid expressing rapsyn–GFP were treated in the absence (*Control*) or presence of 10 or 20 mM MβCD for 1 hr at 37°C and then fixed, permeabilized, and incubated with filipin to detect cholesterol (see Materials and Methods). In control experiments, rapsyn–GFP- and filipin-derived free cholesterol signals showed significant colocalization at the plasma membrane (*short arrows*), in vesicular structures (*long arrows*), and in the juxtanuclear region (*arrowheads*). Cholesterol depletion by MβCD perturbed the subcellular localization of rapsyn–GFP. In cells treated with 10 mM MβCD, rapsyn–GFP signal appeared dispersed within the cytoplasm. On higher MβCD concentrations (20 mM) providing acute cholesterol depletion, rapsyn–GFP was dramatically redistributed and appeared diffuse in the cytoplasm. Scale bar, 10 μm.

(*lanes 9–12*). Rapsyn–GFP and AChR expressed separately (Fig. 8*B*,*C*) or together (Fig. 8*A*) have a similar distribution: both are enriched in the low-density raft fractions. These observations indicate that rapsyn and AChR segregate independently within lipid raft microdomains in COS-7 cells.

To strengthen the notion of the participation of the raft machinery in the intracellular trafficking of rapsyn and AChR along the exocytic pathway, we evaluated the cholesterol requirements of competent membranes in COS-7 cells. We localized the subcellular pools of free cholesterol with the fluorescent antibiotic filipin. Rapsyn–GFP and the filipin-derived free cholesterol fluorescences showed similar distributions and significant colocalization at the plasma membrane (Fig. 9, *Control*, *arrowheads*), in vesicular structures, and in a dense juxtanuclear area (Fig. 9, *Control*, *arrows*). A juxtanuclear accumulation of cholesterol using filipin fluorescence similar to the present observation was reported previously to correspond to the Golgi complex (McCabe and Berthiaume, 1999). In a second series of experiments, we depleted COS-7 of cholesterol using MβCD. In cells treated with 10 mM MβCD, rapsyn–GFP appeared more dispersed within the cytoplasm, in agreement with the partial transformation of the Golgi complex/TGN into dispersed 100–200 nm vesicles (Hansen et al., 2000). At the cell surface, rapsyn clusters were no longer visible at the plasma membrane, the fluorescent signal being more homogeneous (less punctated), as compared with control cells (Fig. 9). The efficiency of MβCD treatment in the removal of free cholesterol was monitored by filipin fluorescence. A reduced signal intensity was observed as compared with control cells (Fig. 9). When cells were treated with higher MβCD concentrations (20 mM), we observed an even more dramatic redistribution of rapsyn–GFP concomitant with a massive cholesterol depletion (Fig. 9). Collectively, these data are consistent with the notion that lipid raft microdomains may account for the sorting of rapsyn and AChR within the exocytic pathway and govern their subsequent delivery and clustering at the plasma membrane.

## DISCUSSION

In this study, we showed that neosynthesized rapsyn initially associates with the *trans*-Golgi network and is subsequently targeted via vesiculotubular organelles to the plasma membrane in COS-7 cells. Cotransfection experiments of rapsyn and AChR subunits support the notion that these two molecules are cotargeted via the exocytic pathway to the cell surface. Furthermore, rapsyn and AChR are inserted within cholesterol–sphingolipids raft microdomains. This led us to postulate that sorting, delivery, and final localization of these two proteins to the plasma membrane might be mediated by a protein segregation mechanism within lipid raft microdomains. These basic mechanisms are likely to participate in the accumulation of synaptic AChR, as well as signaling proteins at the neuromuscular junction.

The present observation that the myristoylated protein rapsyn associates initially with membranes in the exocytic pathway before its subsequent targeting to the plasma membrane is in agreement with several reports. The acylation of the Src-related tyrosine kinase p56Lck (Bijlmakers and Marsh, 1999), of the neurospecific calmodulin-binding protein growth-associated protein 43 (Liu et al., 1994), and of the soluble *N*-ethylmaleimide-sensitive factor attachment protein receptor protein synaptosome-associated protein 25 (Gonzalo and Linder, 1998) is required not only for their association with subcellular compartments but also for targeting to their proper destination. Moreover, the targeting to the cell surface and palmitoylation of these proteins are prevented by brefeldin A, indicating that intracellular trafficking of these acylated proteins depends on a functional secretory pathway (Liu et al., 1994; Gonzalo and Linder, 1998; Bijlmakers and Marsh, 1999). Along the same line, the initial targeting of the palmitoylated PSD-95 protein to a perinuclear membranous compartment appeared necessary for both its synaptic targeting and NMDA receptor clustering (El-Husseini et al., 2000). Collectively, these data highlight the crucial role of the exocytic pathway in the sorting and targeting of peripheral acylated proteins to their proper membrane domains.

Increasing evidence suggests that nicotinic AChRs are associated directly or via linker proteins with the raft machinery. The lipid composition of purified AChR-enriched *Torpedo* postsynap-

tic membranes highlighted the prominence of cholesterol and long-chain fatty acyl constituents (Popot et al., 1978). On the other hand, it has been shown that the functional properties of AChR are modulated by its lipid microenvironment, notably cholesterol (for review, see Barrantes, 1997). In addition, Roccamo et al. (1999) showed that cells defective in sphingolipid biosynthesis express low amounts of muscle AChR at the surface membrane, suggesting that sphingolipid metabolism may influence the trafficking of the protein. Recently, Brusés et al. (2001) reported that membrane rafts are necessary for the formation and maintenance of $\alpha$7 nicotinic AChR clusters in somatic spines of ciliary neurons. On the other hand, in addition to their well characterized role as hydrophobic anchors for otherwise soluble proteins, covalent lipid modifications appear to be important determinants of the lateral distribution of proteins in subdomains of the plasma membrane (Brown and London, 1998; Dunphy and Linder, 1998). Recent reports highlighted the fact that several acylated proteins, including singly myristoylated ones, are selectively recruited to liquid-ordered cholesterol and glycosphingolipid-enriched membrane microdomains (Schroeder et al., 1994, 1998; Song et al., 1997; Arni et al., 1998; Michaely et al., 1999; Lindwasser and Resh, 2001; McCabe and Berthiaume, 2001). Being myristoylated, rapsyn may potentially associate with lipid rafts on its own. Such data led us to test the hypothesis of the association of the myristoylated protein rapsyn and AChR with lipid rafts. The detection of these two molecules within low-density, detergent-resistant fractions on sucrose gradient, together with the immunocytochemical colocalization of rapsyn–GFP with subcellular cholesterol-enriched structures, suggested their association with lipid microdomains in COS-7 cells. Ongoing experiments from our laboratory indicate that lipid rafts may also participate in AChR intracellular trafficking in myocytes (F. Stetzkowski-Marden, S. Marchand, and J. Cartaud, unpublished observations). Rafts are viewed as dynamic lipidic domains involved in sorting, vesicle formation, and movement, as well as in vesicle docking and fusion. These domains can selectively incorporate or exclude proteins and thereby govern protein–protein and protein–lipid interaction (for review, see Ikonen, 2001). Given the well established function of rafts in protein sorting, it is likely that neosynthesized rapsyn is selectively targeted to an exocytic pathway after segregation with local lipid raft microdomains. We also observed that AChR or rapsyn incorporates within lipid rafts when expressed independently, thus suggesting that rapsyn is not necessary for proper segregation of its companion receptor within raft microdomains**.** These data are in agreement with our observations that rapsyn expression does not modify the intracellular routes followed by the AChR. It has been proposed that in polarized epithelial cells, lipid raft domains selectively mediate apical protein and lipid localizations (for review, see Simons and Ikonen, 1997). Additional studies in such polarized cells should give new insights regarding the participation of rafts in the respective targeting of AChR and associated proteins to specialized membrane domains. Finally, our data are consistent with increasing evidence suggesting that other neurotransmitter receptors, such as AMPA-type glutamate receptors, are associated directly or via linker proteins with the cholesterol-rich membrane microdomain rafts (Bruckner et al., 1999; Suzuki et al., 2001).

Time-lapse imaging and immunoelectron microscopy highlighted the fact that large pleiomorphic vesiculotubular structures, rather than small vesicles, were found to be the primary vehicles for post-Golgi to plasma membrane transport of rapsyn–GFP. This observation is consistent with recent works reporting that a unifying vesicular paradigm for transport intermediates was no longer sustainable. Vesicular–tubular clusters rather than isolated vesicles have been shown to operate as intermediates between the ER and the Golgi complex, and tubules have been suggested to mediate intra-Golgi, retrograde Golgi-to-ER, and TGN to plasma membrane transports (for review, see Lippincott-Schwartz et al., 2000; Polishchuk et al., 2000).

Rapsyn was observed as large fluorescent dots colocalizing with AChR not only at the plasma membrane but also within the cytoplasm in association with exocytic compartments. This pattern suggests that AChR and rapsyn are already accumulated within vesiculotubular carriers, as observed for other cargo protein in transit (Hirschberg et al., 1998). Rapsyn has the property to self-associate and consequently could oligomerize after association with intracellular membrane lipid rafts. Lipid rafts are known to facilitate protein–protein interactions by segregating proteins and lipids, so the localization of rapsyn and AChR within these raft microdomains could account for their microclustering before their macro-clustering at the cell surface. The present study, together with our recent demonstration that components of the dystrophin-associated protein complex are cotargeted with AChR and rapsyn via the same post-Golgi vesicles to the *Torpedo* postsynaptic membrane (Marchand et al., 2001), supports the notion of a targeted delivery of prefabricated complexes to synaptic sites. In addition, the assembly of signaling synaptic molecules together with AChR and rapsyn within lipidic rafts may represent an important step in the biogenesis of the postsynaptic apparatus (Stetzkowski-Marden, Marchand, and Cartaud, unpublished observations).

Increasing evidence shows that the organization of cytoskeletal elements, and in particular that of microtubules, facilitates the targeted delivery of TGN-derived transport vesicles for long-distance carriage toward the appropriate membrane domain (Mays et al., 1994; Lafont and Simons, 1996). Videomicroscopy analysis demonstrated the participation of the microtubular network in the localization and transport of rapsyn–GFP in COS-7 cells. The linear trajectory and the speed of the transport (0.2 $\mu$m/sec) are concordant with a kinesin-guided movement along microtubules. These data are in agreement with previous observations suggesting that the cotargeting of AChR and rapsyn to the neuromuscular junction could be contributed by a microtubule-dependent vectorial delivery along the exocytic pathway (Jasmin et al., 1990; Bignami et al., 1998; Camus et al., 1998; Marchand et al., 2000). Several recent reports point to the notion that scaffolding and anchoring proteins [gephyrin and GABA type A receptor-associated protein (H. B. Wang et al., 1999; Kneussel et al., 2000; Kittler et al., 2001) and PSD-95 (El-Husseini et al., 2000)] participate in the association of receptor complex-containing vesicular transporters with microtubules. Whether rapsyn plays a similar role for AChR vesicular trafficking remains to be explored.

The present data are in agreement with the view that several postsynaptic proteins [PSD-95 (El-Husseini et al., 2000), SAP97 (Sans et al., 2001), stargazin (Chen et al., 2000; for review, see Tomita et al., 2001), and GRIP (Dong et al., 1999)] involved in the clustering and scaffolding of NMDA or AMPA glutamate receptors at the postsynaptic sites might associate initially with the exocytic pathway. These data emphasize that these proteins are not merely static cytoskeletal elements but are itinerant proteins involved in transport of receptor-containing vesicles destined to be conveyed to their appropriate synaptic site. One can

postulate an additional dynamical role of this class of proteins in the targeting of neurotransmitter receptors along the biosynthetic pathway. From the present experiments limited to COS cells, we cannot conclude that rapsyn participates in the regulation of the intracellular trafficking of AChR. Additional experiments in muscle cells are thus needed to elucidate this point.

## REFERENCES


Arni S, Keilbaugh SA, Ostermeyer AG, Brown DA (1998) Association of GAP-43 with detergent-resistant membranes requires two palmitoylated cysteine residues. J Biol Chem 273:28478–28485.

Banting G, Ponnambalam S (1997) TGN38 and its orthologues: roles in post-TGN vesicle formation and maintenance of TGN morphology. Biochim Biophys Acta 1355:209–217.

Barrantes FJ (1997) The acetylcholine receptor ligand-gated channel as a molecular target of disease and therapeutic agents. Neurochem Res 22:391–400.

Bignami F, Camus G, Marchand S, Bailly L, Stetzkowski-Marden F, Cartaud J (1998) Targeting of acetylcholine receptor and 43 kDa rapsyn to the postsynaptic membrane in *Torpedo marmorata* electrocyte. J Physiol (Paris) 92:177–181.

BijImakers MJJE, Marsh M (1999) Trafficking of an acylated cytosolic protein: newly synthetized p56lck travels to the plasma membrane via the exocytic pathway. J Cell Biol 145:457–468.

Brown DA, London E (1998) Functions of lipid rafts in biological membranes. Annu Rev Cell Dev Biol 14:111–136.

Bruckner K, Pablo Labrador J, Scheiffele P, Herb A, Seeburg PH, Klein R (1999) EphrinB ligands recruit GRIP family PDZ adaptor proteins into raft membrane microdomains. Neuron 22:511–524.

Brusés JL, Chauvet N, Rutishauser U (2001) Membrane lipid rafts are necessary for the maintenance of the (α)7 nicotinic acetylcholine receptor in somatic spines of ciliary neurons. J Neurosci 21:504–512.

Camus G, Jasmin BJ, Cartaud J (1998) Polarized sorting of nicotinic acetylcholine receptors to the postsynaptic membrane in Torpedo electrocyte. Eur J Neurosci 10:839–852.

Cartaud A, Stetzkowski-Marden F, Cartaud J (1993) Identification of dystrophin-binding proteins in membranes from *Torpedo* electrocyte and rat muscle. J Biol Chem 268:13019–13022.

Chardin P, McCormick F (1999) Brefeldin A: the advantage of being uncompetitive. Cell 97:153–155.

Chavrier P, Parton RG, Hauri HP, Simons K, Zerial M (1990) Localization of low molecular weight GTP binding proteins to exocytic and endocytic compartments. Cell 62:317–329.

Chen L, Chetkovich DM, Petralia RS, Sweeney NT, Kawasaki Y, Wenthold RJ, Bredt DS, Roger AN (2000) Stargazin regulates synaptic targeting of AMPA receptors by two distinct mechanisms. Nature 408:936–943.

Dong H, Zhang P, Liao D, Huganir RL (1999) Characterization, expression, and distribution of GRIP protein. Ann NY Acad Sci 868:535–540.

Dunphy JT, Linder ME (1998) Signalling functions of protein palmitoylation. Biochim Biophys Acta 1436:245–261.

El-Husseini AE, Craven SE, Chetkovich DM, Firestein BL, Schnell E, Aoki C, Bredt DS (2000) Dual palmitoylation of PSD-95 mediates its vesiculotubular sorting, postsynaptic targeting, and ion channel clustering. J Cell Biol 148:159–172.

Froehner SC, Luetje CW, Scotland PB, Patrick J (1990) The postsynaptic 43K protein clusters muscle nicotinic acetylcholine receptors in *Xenopus* oocytes. Neuron 5:403–410.

Gautam M, Noakes PG, Mudd J, Nichol M, Chu GC, Sanes JR, Merlie JP (1995) Failure of postsynaptic specialization to develop at neuromuscular junctions of rapsyn-deficient mice. Nature 377:232–236.

Gonzalo S, Linder ME (1998) SNAP-25 palmitoylation and plasma membrane targeting require a functional secretory pathway. Mol Biol Cell 9:585–597.

Griffiths G, Hoflack B, Simons K, Mellman I, Kornfeld S (1988) The mannose 6-phosphate receptor and the biogenesis of lysosomes. Cell 52:329–341.

Hansen GH, Niels-Christiansen LL, Thorsen E, Immerdal L, Danielsen EM (2000) Cholesterol depletion of enterocytes. Effect on the Golgi complex and apical membrane trafficking. J Biol Chem 275:5136–5142.

Hirschberg K, Miller CM, Ellenberg J, Presley JF, Siggia ED, Phair RD, Lippincott-Schwartz J (1998) Kinetic analysis of secretory protein traffic and characterization of Golgi to plasma membrane transport intermediates in living cells. J Cell Biol 143:1485–1503.

Horn M, Banting G (1994) Okadaic acid treatment leads to a fragmentation of the *trans*-Golgi network and an increase in expression of TGN38 at the cell surface. Biochem J 301:69–73.

Ikonen E (2001) Roles of lipid rafts in membrane transport. Curr Opin Cell Biol 13:470–477.

Jasmin BJ, Cartaud J, Bornens M, Changeux JP (1989) Golgi apparatus in chick skeletal muscle: changes in its distribution during end plate development and after denervation. Proc Natl Acad Sci USA 86:7218–7222.

Jasmin BJ, Changeux JP, Cartaud J (1990) Compartmentalization of cold-stable and acetylated microtubules in the subsynaptic domain of chick skeletal muscle fibre. Nature 344:673–675.

Kittler JT, Rostaing P, Schiavo G, Fritschy JM, Olsen R, Triller A, Moss SJ (2001) The subcellular distribution of GABARAP and its ability to interact with NSF suggest a role for this protein in the intracellular transport of GABAA receptors. Mol Cell Neurosci 18:13–25.

Kneussel M, Haverkamp S, Fuhrmann JC, Wang H, Wassle H, Olsen RW, Betz H (2000) The gamma-aminobutyric acid type A receptor (GABAAR)-associated protein GABARAP interacts with gephyrin but is not involved in receptor anchoring at the synapse. Proc Natl Acad Sci USA 97:8594–8599.

Lafont F, Simons K (1996) The role of microtubule-based motors in the exocytic transport of polarized cells. Semin Cell Dev Biol 7:343–355.

Lindwasser OW, Resh MD (2001) Multimerization of human immunodeficiency virus type 1 Gag promotes its localization to barges, raft-like membrane microdomains. J Virol 75:7913–7924.

Liou W, Geuze HJ, Slot JW (1996) Improving structural integrity of cryosections for immunogold labeling. Histochemistry 106:41–58.

Lippincott-Schwartz J, Roberts TH, Hirschberg K (2000) Secretory protein trafficking and organelle dynamics in living cells. Annu Rev Cell Dev Biol 16:557–589.

Liu Y, Fischer DA, Storm DR (1994) Intracellular sorting of neuromodulin (GAP-43) mutants modified in the membrane targeting domains. J Neurosci 14:5807–5817.

Marchand S, Bignami F, Stetzkowski-Marden F, Cartaud J (2000) The myristoylated protein rapsyn is cotargeted with the nicotinic acetylcholine receptor to the postsynaptic membrane via the exocytic pathway. J Neurosci 20:521–528.

Marchand S, Stetzkowski-Marden F, Cartaud J (2001) Differential targeting of components of the dystrophin complex to the postsynaptic membrane. Eur J Neurosci 13:221–229.

Mays RW, Beck KA, Nelson WJ (1994) Organization and function of the cytoskeleton in polarized epithelial cells: a component of the protein sorting machinery. Curr Opin Cell Biol 6:16–24.

McCabe JB, Berthiaume LG (1999) Functional roles for fatty acylated amino-terminal domains in subcellular localization. Mol Biol Cell 10:3771–3786.

McCabe JB, Berthiaume LG (2001) N-terminal protein acylation confers localization to cholesterol, sphingolipid-enriched membranes but not to lipid rafts/caveolae. Mol Biol Cell 12:3601–3617.

Michaely PA, Mineo C, Ying Y, Anderson RGW (1999) Polarized distribution of endogenous Rac1 and RhoA at the cell surface. J Biol Chem 274:21430–21436.

Muller CP, Stephany DA, Winkler DF, Hoeg JM, Demosky Jr SJ, Wunderlich JR (1984) Filipin as a flow microfluorometry probe for cellular cholesterol. Cytometry 5:42–54.

Musil LS, Carr C, Cohen JB, Merlie JP (1988) Acetylcholine receptor-associated 43 K protein contains covalently bound myristate. J Cell Biol 107:1113–1121.

Phillips WD, Kopta C, Blount P, Gardner PD, Steinbach JH, Merlie JP (1991a) ACh receptor-rich domains organized in fibroblasts by recombinant 43-kilodalton protein. Science 251:568–570.

Phillips WD, Maimone MM, Merlie JP (1991b) Mutagenesis of the 43 kD postsynaptic protein defines domains involved in plasma membrane targeting and AChR clustering. J Cell Biol 115:1713–1723.

Polishchuk RS, Polishchuk EV, Marra P, Alberti S, Buccione R, Luini A, Mironov AA (2000) Correlative light-electron microscopy reveals the tubular-saccular ultrastructure of carriers operating between Golgi apparatus and plasma membrane. J Cell Biol 148:45–58.

Ponnambalam S, Girotti M, Yaspo ML, Owen CE, Perry AC, Suganuma T, Nilsson T, Fried M, Banting G, Warren G (1996) Primate homologues of rat TGN38: primary structure, expression and functional implications. J Cell Sci 109:675–685.

Popot JL, Demel RA, Sobel A, Van Deenen LL, Changeux JP (1978) Interaction of the acetylcholine (nicotinic) receptor protein from *Torpedo marmorata* electric organ with monolayers of pure lipids. Eur J Biochem 85:27–42.

Ramarao MK, Cohen JB (1998) Mechanism of nicotinic acetylcholine receptor cluster formation by rapsyn. Proc Natl Acad Sci USA 95:4007–4012.

Ramarao MK, Bianchetta MJ, Lanken J, Cohen JB (2001) Role of rapsyn tetratricopeptide repeat and coiled-coil domains in self-association and nicotinic acetylcholine receptor clustering. J Biol Chem 276:7475–7483.

Raposo G, Kleijmeer MJ, Posthuma G, Slot JW, Geuze HJ (1997) Immunogold labeling of ultrathin cryosections: application in immunology. In: Weir's handbook of experimental immunology, Ed 5 (Blackwell I, ed), pp 1–11. Cambridge, MA: Elsevier.

Resh MD (1999) Fatty acylation of proteins: new insights into membrane targeting of myristoylated and palmitoylated proteins. Biochim Biophys Acta 1451:1–16.

Roccamo AM, Pediconi MF, Aztiria E, Zanello L, Wolstenholme A,

Barrantes FJ (1999) Cells defective in sphingolipids biosynthesis express low amounts of muscle nicotinic acetylcholine receptor. Eur J Neurosci 11:1615–1623.
Sanes JR, Lichtman JW (1999) Development of the vertebrate neuromuscular junction. Annu Rev Neurosci 22:389–442.
Sans N, Racca C, Petralia RS, Wang YX, McCallum J, Wenthold RJ (2001) Synapse-associated protein 97 selectively associates with a subset of AMPA receptors early in their biosynthetic pathway. J Neurosci 21:7506–7516.
Schaeffer L, de Kerchove d'Exaerde A, Changeux J-P (2001) Targeting transcription to the neuromuscular synapse. Neuron 31:15–22.
Schroeder R, London E, Brown D (1994) Interactions between saturated acyl chains confer detergent resistance on lipids and glycosylphosphatidylinositol (GPI)-anchored proteins: GPI-anchored proteins in liposomes and cells show similar behavior. Proc Natl Acad Sci USA 91:12130–12134.
Schroeder RJ, Ahmed SN, Zhu Y, London E, Brown DA (1998) Cholesterol and sphingolipid enhance the Triton X-100 insolubility of glycosylphosphatidylinositol-anchored proteins by promoting the formation of detergent-insoluble ordered membrane domains. J Biol Chem 273:1150–1157.
Sciaky N, Presley J, Smith C, Zaal KJ, Cole N, Moreira JE, Terasaki M, Siggia E, Lippincott-Schwartz J (1997) Golgi tubule traffic and the effects of brefeldin A visualized in living cells. J Cell Biol 139:1137–1155.
Simons K, Ikonen E (1997) Functional rafts in cell membranes. Nature 387:569–572.
Slot JW, Geuze HJ, Gigengack S, Lienhard GE, James D (1991) Immunolocalization of the insulin regulatable glucose transporter in brown adipose tissue of the rat. J Cell Biol 113:123–135.
Sobel A, Weber M, Changeux J-P (1977) Large-scale purification of the acetylcholine receptor protein in its membrane-bound and detergent-extracted forms from *Torpedo marmorata* electric organ. Eur J Biochem 80:215–224.
Song KS, Sargiacomo M, Galbiati F, Parenti M, Lisanti MP (1997) Targeting of a G alpha subunit (Gi1 alpha) and c-Src tyrosine kinase to caveolae membranes: clarifying the role of *N*-myristoylation. Cell Mol Biol 43:293–303.
Suzuki T, Ito J, Takagi H, Saitoh F, Nawa H, Shimizu H (2001) Biochemical evidence for localization of AMPA-type glutamate receptor subunits in the dendritic raft. Brain Res Mol Brain Res 89:20–28.
Tartakoff AM, Vassalli P (1983) Lectin-binding sites as markers of Golgi subcompartments: proximal-to-distal maturation of oligosaccharides. J Cell Biol 97:1243–1248.
Tomita S, Nicoll RA, Bredt DS (2001) PDZ protein interactions regulating glutamate receptor function and plasticity. J Cell Biol 153:F19–F24.
Towbin H, Staehelin T, Gordon J (1979) Electrophoresis transfer of proteins from polyacrylamide gels to nitrocellulose sheets: procedure and some applications. Proc Natl Acad Sci USA 76:4350–4354.
Wang HB, Bedford FK, Brandon NJ, Moss SJ, Olsen RW (1999) $GABA_A$-receptor-associated protein links $GABA_A$ receptors and the cytoskeleton. Nature 397:69–72.
Wang ZZ, Mathias A, Gautam M, Hall ZW (1999) Metabolic stabilization of muscle nicotinic acetylcholine receptor by rapsyn. J Neurosci 19:1998–2007.
Watson RT, Pessin JE (2000) Functional cooperation of two independent targeting domains in syntaxin 6 is required for its efficient localization in the *trans*-Golgi network of 3T3L1 adipocytes. J Biol Chem 275:1261–1268.
Yu XM, Hall ZW (1994) The role of the cytoplasmic domains of individual subunits of the acetylcholine receptor in 43 kDa protein-induced clustering in COS cells. J Neurosci 14:785–795.